

Are your **MRI contrast agents** cost-effective?

Learn more about generic **Gadolinium-Based Contrast Agents**.



**FRESENIUS  
KABI**

caring for life

**AJNR**

## **Contrast-Enhanced MR Angiography of the Carotid and Vertebrobasilar Circulations**

Carina W. Yang, James C. Carr, Stephen F. Futterer, Mark D. Morasch, Benson P. Yang, Stephanie M. Shors and J. Paul Finn

This information is current as of April 19, 2024.

*AJNR Am J Neuroradiol* 2005, 26 (8) 2095-2101  
<http://www.ajnr.org/content/26/8/2095>

## Contrast-Enhanced MR Angiography of the Carotid and Vertebrobasilar Circulations

Carina W. Yang, James C. Carr, Stephen F. Futterer, Mark D. Morasch, Benson P. Yang, Stephanie M. Shors, and J. Paul Finn

**BACKGROUND AND PURPOSE:** Contrast-enhanced MR angiography (CE MRA) is a proven diagnostic tool in evaluation of the carotid arteries; however, few studies have addressed its accuracy in the vertebrobasilar system. The purpose of this study was to assess the sensitivity and specificity of CE MRA compared with digital subtraction angiography (DSA) for detection of vertebrobasilar disease.

**METHODS:** Forty patients with suspected atherosclerotic disease of the carotid and vertebrobasilar circulations underwent CE MRA on a 1.5T MR imaging scanner by use of a coronal 3D gradient-echo pulse sequence after intravenous injection of gadolinium diethylene triamine penta-acetic acid. All patients had correlative DSA within a 1-month period. CE MRA images were randomized and then independently assessed by 2 observers who were blinded to the DSA results. DSA examinations were analyzed in a similar manner. Each observer was asked to report the presence or absence of clinically significant stenosis (>50%), occlusion, fistula, aneurysm, and dissection. The MRA findings were then correlated with DSA.

**RESULTS:** The sensitivity and specificity of MRA for detection of disease in the entire carotid and vertebrobasilar systems were 90% and 97%, respectively; for the carotid system alone, the sensitivity and specificity were 94% and 97%, respectively; and for the vertebrobasilar system they were 88% and 98% respectively. The overall interobserver reliability was 98% ( $\kappa = 0.92$ ).

**CONCLUSION:** CE MRA is accurate at detecting disease not only in the carotid vessels, but also in the vertebrobasilar circulation, and has the potential to provide a comprehensive and noninvasive evaluation of the head and neck arteries in a single study.

Atherosclerotic disease of the carotid and vertebral arteries is a major cause of stroke, affecting more than 500,000 individuals annually in the United States and often leading to permanent disability (1). Disease in the vertebrobasilar system, however, has potentially more lethal consequences, resulting in stroke within the brainstem, which is commonly fatal. It is important to assess both the carotid and vertebrobasilar circulation, first to ascertain the exact source of neurologic symptoms and second to decide whether lesions are potentially amenable to surgical or endovascular treatment (2–7). Digital subtraction angiog-

raphy (DSA) has traditionally been the gold standard for evaluating the carotid and vertebral arteries. It is, however, an invasive procedure associated with some morbidity and mortality (8–10).

Contrast-enhanced MR angiography (CE MRA) has recently emerged as an alternative, noninvasive technique for assessing vascular disease and is now routinely used as a first-line investigation in different parts of the body (11–15). Vertebrobasilar disease has posed a more difficult challenge for MRA, mainly because of the smaller size of the vessels involved (16). Initial attempts to assess the vertebrobasilar system with MRA employing time-of-flight (TOF) techniques yielded good results for detection of arterial disease (17–22). Acquisition times, however, were long, and this resulted in significant image degradation due to motion artifact. Because of the larger anatomic coverage and improved image quality, CE MRA quickly superseded TOF as the method of choice for imaging the cervical vessels. During the past decade, CE MRA has become an established diagnostic tool for evaluating the supraaortic vessels (16, 23–27), with high sensitivities and specificities reported for detection of carotid artery stenosis (17,

---

Received November 1, 2004; accepted after revision February 10, 2005.

From the Departments of Radiology (C.W.Y., J.C.C., S.F.F.), Vascular Surgery (M.D.M.), and Neurological Surgery (B.P.Y.), Northwestern University Feinberg School of Medicine, and Department of Radiology and Nuclear Medicine, Rush University Medical Center (S.M.S.), Chicago, IL; and the Department of Radiological Sciences, UCLA Medical Center (J.P.F.), Los Angeles, CA.

Address correspondence to Carina W. Yang, MD, Department of Radiology, Northwestern University Feinberg School of Medicine, 676 North St. Clair Street, Chicago, IL 60611.

28–34). More recently, it has been shown that high-resolution breath-hold CE MRA can produce high-quality images of the entire carotid and vertebrobasilar circulations in a single acquisition (18, 35–37). Furthermore, CE MRA has been shown to be a promising tool for imaging the extracranial and intracranial portions of vertebral arteries, especially for assessing serial changes following an acute dissection (38). To date, however, no single study has specifically addressed the overall accuracy of CE MRA for detecting clinically significant disease in the vertebrobasilar system.

The purpose of this study was to assess the sensitivity and specificity of high-resolution breath-hold CE MRA compared with DSA for detection of vertebrobasilar disease in a group of 40 patients.

## Materials and Methods

### Patients

CE MRA examinations of the neck vessels carried out during a 2-year period from January 1, 2001, to December 31, 2002, were retrospectively reviewed on a PACS workstation (GE Medical Systems, Milwaukee, WI). Patients who had undergone CE MRA and DSA within 1 month of each other were included in the study. Patients without correlative DSA within a 1-month period were excluded from the study. In addition, 22 subjects were excluded because selective DSA was performed that did not include both bilateral carotid and vertebral injections; 4 subjects were excluded because not all required images were available; 3 subjects were excluded because only TOF images, rather than CE MRA images, were obtained; and one subject was excluded because of a poor signal intensity-to-noise ratio (SNR). This resulted in a cohort of 40 patients (23 men, 17 women; age range, 22–94 years; mean age,  $55 \pm 18$  years, 5 months) and this formed the study group. The clinical indications for MRA and DSA were as follows: posterior circulation symptoms ( $n = 13$ ); anterior/middle circulation symptoms ( $n = 16$ ); nonspecific symptoms ( $n = 11$ ). This study was carried out in accordance with institutional review board guidelines.

### CE MRA Technique

CE MRA studies were performed on a 1.5T Magnetom Symphony (Siemens Medical Systems, Iselin, NJ). Before positioning the patient, a 20-gauge cannula was inserted into an antecubital vein and connected via extendable tubing to a power injector (Medrad, Indianola, PA) containing 20 mL of gadopentate dimeglumine (Magnevist; Berlex Laboratories, Montvale, NJ) and 40 mL of normal saline. Patients were placed in a supine position on the scan table, and a single circularly polarized standard neck coil was connected. They were then entered headfirst into the magnet bore.

A preliminary 2-dimensional (2D) timing-bolus acquisition was obtained in the coronal plane, to include the aortic arch up to the intracerebral circulation. Two milliliters of gadopentate dimeglumine was injected at 2 mL/s followed by a 20-mL bolus of normal saline. The transit time was recorded as the time between the start of the injection and initial enhancement of the carotid bifurcation.

A coronal 3D gradient-echo fast low-angle shot (FLASH) pulse sequence with asymmetric k-space acquisition in all 3 gradient axes was used for high-resolution CE MRA; the remainder of k-space was filled with zero padding. The FLASH sequence had scanning parameters as follows: TR/TE, 4.36/1.64; flip angle, 25°; bandwidth, 432 Hz; matrix,  $136 \times 512$ ; field of view,  $165 \times 330$  mm; slab thickness, 70 mm; partitions, 80;

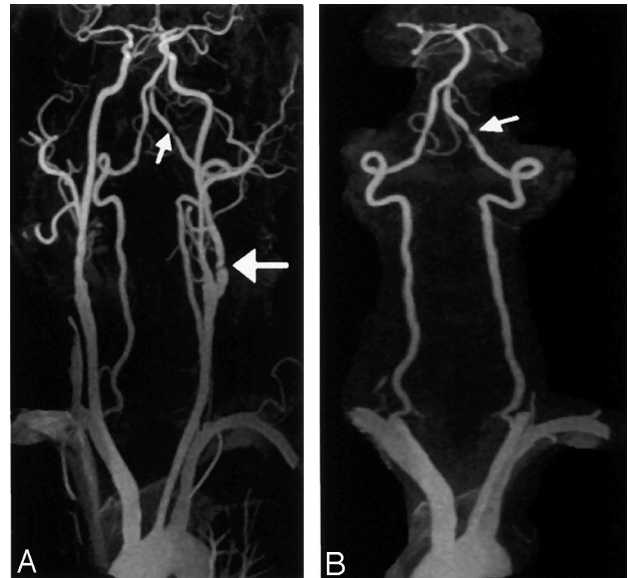


FIG 1. A 72-year-old man with suspected carotid artery disease.

A, CE MRA of the carotid and vertebrobasilar circulations (3D FLASH, TR/TE, 4.36/1.64; flip angle 25°; bandwidth, 432 Hz; matrix  $136 \times 512$ ; field of view,  $165 \times 330$  mm; slab thickness, 70 mm; partitions, 80; and voxel size,  $1.33 \times 0.64 \times 1.15$  mm<sup>3</sup>) shows stenoses in proximal left internal carotid artery (large arrow) and distal left vertebral artery (small arrow).

B, CE MRA MIP image, with carotid vessels edited out, more clearly shows the left vertebral artery stenosis (arrow).

and voxel size,  $1.33 \times 0.64 \times 1.15$  mm<sup>3</sup>. Acquisition time was approximately 19 seconds per 3D slab. After obtaining the initial timing bolus, 20 mL of gadolinium diethylene triamine penta-acetic acid were then injected at 2 mL/s. Patients were asked to hyperventilate before scanning began and to hold their breath on inspiration during image acquisition. All patients held their breath successfully. Pre- and postcontrast breath-held 3D volumes were acquired in a coronal orientation, extending from the aortic arch up through the intracerebral circulation. In-line digital subtraction was carried out, yielding one subtracted 3D set, as shown in Fig 1A. This was then subjected to a maximum intensity projection (MIP) postprocessing algorithm. All images were of diagnostic quality.

A MIP of the entire carotid and vertebrobasilar circulation was provided. Each carotid was displayed separately by manually editing away the other vessels. A MIP of the vertebrobasilar circulation in isolation (Fig 1B) was obtained by manually editing out the carotids.

All postprocessing was carried out by an experienced MR imaging technologist, with a processing time of approximately 10 minutes per patient.

### DSA Technique

DSA was carried out by using the standard Seldinger technique. The common femoral artery was accessed with a vascular puncture needle and an arterial sheath inserted. Arch angiography was initially performed through a pigtail catheter positioned in the ascending thoracic aorta. Selective carotid and vertebral angiographies were then carried out by using an angled 5F catheter positioned in the proximal common carotid and vertebral arteries. Anteroposterior and oblique sagittal orientations were obtained for imaging.

### Image Analysis

All partition images and edited MIPs of the right and left carotid, as well as vertebrobasilar circulation in isolation (ro-

tated through 180°, at 5° increments), from each CE MRA were then evaluated independently and in a blinded manner by 2 experienced radiologists (J.C., S.F.). DSA images were randomized and evaluated in a similar manner by a radiologist (S.F.) and vascular surgeon (M.M.). Each observer was asked to report his findings on a standardized diagram of the arterial circulation in the head and neck. The vertebral arteries were divided into 4 segments (V1–V4), the basilar artery into one segment, and the internal carotid into intracranial and extracranial segments.

The presence or absence of disease was noted, including significant atherosclerotic narrowing (defined as stenosis >50%), segmental occlusion, complete occlusion, aneurysm, dissection, or arteriovenous fistula. Percent stenosis on DSA was calculated following caliper measurement of diameters of the normal vessel above the stenosis, as well as at the stenosis, by using the formula: 1/(diameter of normal vessel above stenosis/diameter of vessel at stenosis).

#### Statistical Analysis

The values of sensitivity and specificity were calculated for the presence or absence of overall clinically significant disease. Sensitivity and specificity were also calculated for each disease entity. For each CE MRA, the interobserver reliability was also determined by using the  $\kappa$  coefficient.

### Results

All patients tolerated the procedures well, and image acquisition was successful. All DSA and CE MRA images were of diagnostic quality. DSA of the carotid system detected 7 aneurysms, 1 arteriovenous fistula, 4 dissections, 12 significant stenoses, and 3 occlusions. In the vertebrobasilar system, DSA detected 3 aneurysms, 2 arteriovenous fistulas, 2 dissections, 6 significant stenoses, and 10 occlusions.

The results for detection of stenosis, occlusion, both stenosis and occlusion, and all disease in the carotid and vertebrobasilar circulations are given in Table 1. The interobserver variability for determination of presence or absence of disease is given in Table 2 and was 98% for CE MRA in the carotid arteries ( $\kappa = 0.91$ ) and 98% for CE MRA in the vertebrobasilar circulation ( $\kappa = 0.92$ ). Examples of vertebral artery stenoses and occlusions as seen on CE MRA as compared with selective DSA are shown in Figs 2 and 3. Figure 4 shows CE MRA images of both carotid and vertebrobasilar disease in a single subject, which are confirmed by selective DSA.

### Discussion

This study shows that CE MRA is accurate at detecting clinically significant disease in both the carotid and vertebrobasilar circulations and can provide a comprehensive evaluation of the head and neck vessels from the aortic arch to the circle of Willis in a single study.

DSA has traditionally been the gold standard for assessing atherosclerotic disease of the supraaortic vessels; however, because DSA is an invasive procedure with well-defined morbidity and mortality (8–10), efforts have been made to find a safer, less-invasive tool for evaluating the arterial structures of

**TABLE 1: Sensitivity and specificity of contrast-enhanced MR angiography for the evaluation of disease in the carotid and vertebrobasilar circulations**

	Observer 1		Observer 2	
	Sensitivity (%)	Specificity (%)	Sensitivity (%)	Specificity (%)
Stenosis only				
ICA	88	97	100	99
VB	86	99	100	100
ICA + VB	87	99	100	100
Occlusion only				
ICA	100	100	100	100
VB	83	99	79	99
ICA + VB	86	99	82	99
Stenosis and occlusion				
ICA	92	97	100	99
VB	86	98	87	99
ICA + VB	88	98	91	99
All disease				
ICA	94	97	100	97
VB	88	98	88	99
ICA + VB	90	97	92	98

Note.—ICA indicates internal carotid artery; VB, vertebrobasilar circulation.

**TABLE 2: Interobserver variability of contrast-enhanced MR angiography for the evaluation of stenosis and occlusion in the carotid and vertebrobasilar circulations**

	Interobserver Variability (%)	$\kappa$
ICA	99	0.91
VB	98	0.86
ICA + VB	98	0.92

Note.—ICA indicates internal carotid artery; VB, vertebrobasilar circulation.

the neck. Duplex sonography is routinely used to evaluate the carotid bifurcation but provides little or no information about the vertebrobasilar circulation or great vessel origins. CT angiography (CTA) can be used as an alternative technique to assess the neck vessels, though it uses ionizing radiation and potentially nephrotoxic contrast agent (39–42). In addition, bone artifact in the vertebral column and possibly calcium in the vessel wall may occasionally limit CTA of the vertebral arteries. The next generation of multisection CT scanners, however, has the potential to improve spatial resolution significantly, which will result in more detailed depiction of the carotid and vertebrobasilar vessels.

MRA has emerged as a useful noninvasive technique for assessing vascular disease and is now routinely used in different parts of the body, particularly the carotid circulation. MRA initially was implemented by using 2D and 3D TOF techniques (18–23). These techniques produce satisfactory images of the carotid bifurcation, but long imaging times limit anatomic coverage and result in significant motion artifacts. As a result, the aortic arch, the circle of Willis, and the entire vertebrobasilar circulation are typically

FIG 2. A 65-year-old woman with headache, blurry vision, and arm weakness.

A, CE MRA MIP image (3D FLASH, TR/TE, 4.36/1.64; flip angle 25°; bandwidth, 432 Hz; matrix 136 × 512; field of view, 165 × 330 mm; slab thickness, 70 mm; partitions, 80; and voxel size, 1.33 × 0.64 × 1.15 mm<sup>3</sup>) of the vertebrobasilar system demonstrates severe stenosis at the origin of right vertebral artery (*large arrow*). There is a short segmental occlusion of the distal left vertebral artery (*small arrow*).

B, Selective DSA of right subclavian confirms severe stenosis at the right vertebral origin (*arrow*).

C, Selective DSA of left vertebral artery confirms the distal occlusion (*arrow*).

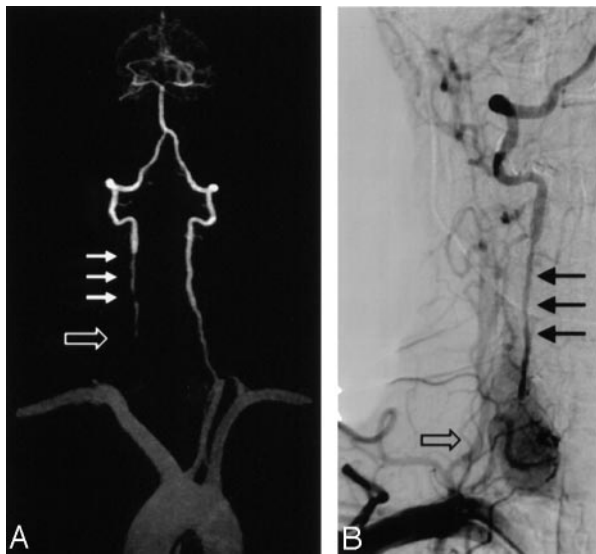


FIG 3. A 46-year-old man with presyncope and right upper extremity weakness.

A, CE MRA MIP image (3D FLASH, TR/TE, 4.36/1.64; flip angle 25°; bandwidth, 432 Hz; matrix 136 × 512; field of view, 165 × 330 mm; slab thickness, 70 mm; partitions, 80; and voxel size, 1.33 × 0.64 × 1.15 mm<sup>3</sup>) of the vertebrobasilar system shows segmental occlusion of the proximal right vertebral artery (*open arrow*), as well as diffuse narrowing superior to the occluded segment (*small arrows*).

B, Selective DSA of the right subclavian confirms occlusion (*open arrow*) and stenosis (*closed arrows*) in proximal right vertebral artery.

not included in the same acquisition. Because of the degradation in image quality, TOF MRA can result in overestimation of the degree of stenosis (43, 44). Even with these limitations, TOF MRA was shown to be a clinically important noninvasive technique for detecting vascular disease in the vertebrobasilar circulation (45, 46). Furthermore, TOF MRA could potentially be more accurate in characterization of occlusive lesions in the vertebrobasilar system than in the carotid circulation (47).

CE MRA has now replaced TOF as the method of choice for imaging the carotid circulation. CE MRA has the ability to consistently produce higher quality, artifact-free images of the head and neck vessels in a much shorter acquisition time. With recent advances in gradient subsystems, it is now possible to achieve shorter repetition times than were previously possible. This results in faster scan times, which allow greater anatomic coverage within a comfortable 20-second acquisition.

A recent study demonstrated the feasibility of high-quality imaging of the entire head and neck circulation, from aortic arch to the circle of Willis, in a single breath-hold CE MRA study (18). This technique was also used in the current study. Because of improved anatomic coverage, previously overlooked atherosclerotic disease outside the carotid bifurcation can now be evaluated. This is important because tandem lesions elsewhere in the carotid circulation may be a significant cause of morbidity in patients with suspected carotid artery disease and may represent the true source of neurologic symptoms (48–53).

In many cases, atherosclerotic disease may occur elsewhere in the carotid system in patients with a normal carotid bifurcation. It is essential to depict the true extent of disease, not only to ascertain the exact etiology of symptoms but also to pinpoint potentially treatable lesions. In the present study, CE MRA was accurate at identifying clinically significant disease within the carotid system from the aortic arch to the circle of Willis. Results are comparable to previously published studies (17, 28–34). Although carotid artery disease is a common and potentially significant cause of debilitation, disease in the vertebrobasilar system may have much more lethal consequences. Brainstem stroke, which can be caused by vertebrobasilar disease, is uncommon, but, when it occurs, it is frequently fatal (54). Furthermore, vertebrobasilar disease is now amenable to successful treatment with surgical reconstruction (55, 56) and newer endovas-

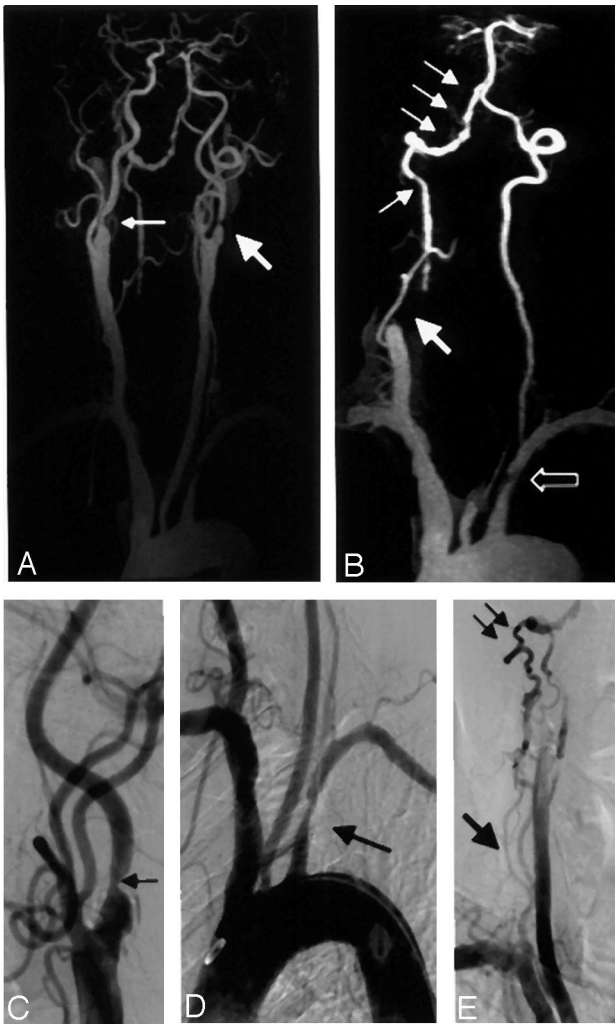


FIG 4. A 59-year-old man with carotid and vertebrobasilar disease.

A, CE MRA coronal MIP (3D FLASH, TR/TE, 4.36/1.64; flip angle 25°; bandwidth, 432 Hz; matrix 136 × 512; field of view, 165 × 330 mm; slab thickness, 70 mm; partitions, 80; and voxel size of 1.33 × 0.64 × 1.15 mm<sup>3</sup>) of the carotid system showing high grade stenosis of the proximal left internal carotid artery (*large arrow*), with moderate stenosis involving the proximal right internal carotid artery (*small arrow*).

B, CE MRA coronal MIP of the vertebrobasilar system with carotid vessels edited away demonstrates segmental occlusion of the right V1 segment (*large arrow*) with reconstitution distally and multifocal stenoses in V3 and V4 segments (*small arrows*). There is also a proximal left subclavian stenosis (*open arrow*).

C, Selective DSA of the right carotid artery confirms stenosis in the proximal right internal carotid (*arrow*).

D, Aortic arch angiography demonstrates focal stenosis of proximal left subclavian artery (*arrow*).

E, Delayed image of DSA run confirms multifocal stenotic disease in the right V3 and V4 segments (*small arrows*), as well as segmental occlusion in the right V1 segment (*large arrow*).

cular techniques (2–7); therefore, it is essential that lesions in this distribution be detected early and accurately.

Although numerous studies have examined the sensitivity and specificity of MRA for detection of carotid artery stenosis (17, 28–34), few have addressed its accuracy in the vertebrobasilar system. Prior studies have shown that MRA is capable of

detecting disease (45, 46), particularly occlusive disease (47), in the vertebrobasilar circulation and may be a useful tool for following vertebral artery dissection (38). Previous studies have not, however, addressed the overall accuracy for detection of atherosclerotic disease in the vertebrobasilar circulation. The vertebral and basilar arteries have been a challenge to image accurately with MRA, primarily because of their small caliber. In addition, because of their posterior anatomic location in the neck, it has been difficult to include them within the coverage of a conventional carotid MRA. The CE MRA technique used in this study allowed for improved anatomic coverage so that the carotid and vertebrobasilar arteries were included in the same acquisition. At the same time, high spatial resolution was maintained, which permitted depiction of the small vertebral arteries.

In this study, the sensitivity and specificity for detection of all disease in the vertebrobasilar circulation were 88% and 98%, respectively. This compared well to the sensitivity and specificity in the carotids alone, which were 94% and 97%, respectively. When significant stenoses and occlusions were considered together, the results again were similar (Table 1). When significant stenoses were considered alone, the sensitivity in the vertebrobasilar was as high as 100% (observer 2). This compared favorably to 100% sensitivity for the carotids alone (also observer 2). Observer 1 missed some significant stenoses in the vertebrobasilar circulation. All of these lesions were located in the V1 segment. This discrepancy may be explained by accentuated pulsatility of the proximal vertebral artery resulting in motion artifact and blurring. Occasional loss of definition of the vertebral artery origins may be due to a small trough in the coil sensitivity at those locations, which is more significant for smaller vessels such as the vertebral artery than for the larger common carotid arteries. This is not, however, a fundamental limitation but more one of coil design that can be addressed in future studies.

All of the occlusions in the carotid vessels were detected by both observers (100% sensitivity). The sensitivity for detection of occlusions was lower in the vertebrobasilar circulation for both observers (83% and 79%, respectively). The likely explanation for this is that CE MRA, because it produces a static image of the vascular structures in time, overestimates the length of the occlusion. DSA, on the other hand, is a dynamic time-resolved technique, which can demonstrate retrograde filling of occluded vertebral artery segments. Therefore, apparent long segmental occlusions on CE MRA may actually be shorter on DSA. The use of time-resolved MRA in the carotids may potentially address this deficiency, and this is the subject of an ongoing study at our institution.

This study has several limitations. First, only patients with DSA and MRA within 1 month of each other were included in the study. This introduces a natural selection bias. The time interval between CE MRA and DSA examinations was chosen to maximize the size of the study group. A time period of 1

month was considered reasonable, because it is expected that there would be no significant disease progression within that time period. Most of the examinations in the study, however, were performed within a shorter time period of <2 weeks. Second, this study had a relatively small number of patients. This is because CE MRA is the first-line tool for evaluating carotid artery disease at our institution. Therefore, only patients with abnormal CE MRAs or discrepant findings on duplex sonography undergo DSA. This also explains the higher incidence of pathology. Third, the sensitivity and specificity of CE MRA in individual vertebral artery segments were not calculated. This was because some vertebral artery segments contained only a single abnormality and it was considered statistically inaccurate to report this. If a larger cohort of patients had been studied, this information could have been included. Fourth, significant stenosis was defined as 50% or greater reduction in luminal diameter. This is clearly at odds with the accepted cutoff of 70% for significant disease, as recommended by NASCET (57, 58). Because the vertebrobasilar circulation was primarily evaluated, a cutoff of 50% was chosen on the basis of accepted determinations of significant stenosis by angiographic criteria (11, 14, 59–62).

Ongoing technological advances promise to improve diagnostic sensitivity for detection of vertebral artery disease. CE MRA at 3T produces a 1.5- to 2-fold increase in SNR compared with 1.5T (63). This SNR gain may be used to improve the spatial resolution. This would be particularly advantageous in the vertebrobasilar system, where the arterial structures are small. In addition, parallel imaging techniques are particularly suited to MRA and can result in more rapid scan times as well as higher spatial resolution. Further advancements in the hardware and software of the next generation of MR imagers will result in even more sophisticated and improved imaging.

## Conclusion

In conclusion, this study confirms that CE MRA is accurate at detecting pathology such as aneurysms and dissections, in addition to stenoses and occlusions not only in the carotid vessels, but also in the vertebrobasilar circulation, and has the potential to provide a comprehensive and noninvasive evaluation of the head and neck arteries in a single study. Breath-hold high-resolution CE MRA could become a diagnostic alternative to DSA in the diagnosis of patients with vertebrobasilar artery disease.

## References

- Kricheff II. Arteriosclerotic ischemic cerebrovascular disease. *Radiology* 1987;162:101–109
- Janssens E, Leclerc X, Gautier C, et al. Percutaneous transluminal angioplasty of proximal vertebral artery stenosis: long-term clinical follow-up of 16 consecutive patients. *Neuroradiology* 2003;46:81–84
- Gupta R, Schumacher H, Mangla S, et al. Urgent endovascular revascularization for symptomatic intracranial atherosclerotic stenosis. *Neurology* 2003;61:1647–1648
- Albuquerque F, Fiorella D, Han P, et al. A reappraisal of angioplasty and stenting for the treatment of vertebral origin stenosis. *Neurosurgery* 2003;53:607–614
- Levy E, Hanel R, Bendok B, et al. Staged stent-assisted angioplasty for symptomatic intracranial vertebrobasilar artery stenosis. *J Neurosurg* 2002;97:1294–1301
- Jenkins J, Subramanian R. Endovascular treatment for vertebrobasilar insufficiency. *Curr Treat Options Cardiovasc Med* 2002;4:385–391
- Nakahara T, Sakamoto S, Hamasaki O, Sakoda K. Stent-assisted angioplasty for intracranial atherosclerosis. *Neuroradiology* 2002;44:706–710
- Heiserman J, Dean B, Hodak J, et al. Neurologic complications of cerebral angiography. *AJNR Am J Neuroradiol* 1994;15:1401–1407
- Waugh JR, Sacharias N. Arteriographic complications in the DSA era. *Radiology* 1992;182:243–246
- Willinsky R, Taylor S, TerBrugge K, et al. Neurologic complications of cerebral angiography: prospective analysis of 2,899 procedures and review of the literature. *Radiology* 2003;227:522–528
- Koelemay M, Lijmer J, Stoker J, et al. Magnetic resonance angiography for the evaluation of lower extremity arterial disease: a meta-analysis. *JAMA* 2001;14:1338–1345
- Grist TM. MRA of the abdominal aorta and lower extremities. *J Magn Reson Imaging* 2000;11:32–43
- Grist TM. Magnetic resonance angiography of renal arterial stenosis. *Coron Artery Dis* 1999;10:151–156
- Holland G, Dougherty L, Carpenter J, et al. Breath-hold ultrafast three-dimensional gadolinium-enhanced MR angiography of the aorta and the renal and other visceral arteries. *AJR Am J Roentgenol* 1996;166:971–981
- Adamis M, Li W, Wielopolski P, et al. Dynamic contrast-enhanced subtraction MR angiography of the lower extremities: initial evaluation with a multisection two-dimensional time-of-flight sequence. *Radiology* 1995;196:689–695
- Wutke R, Lang W, Fellner C, et al. High-resolution, contrast-enhanced magnetic resonance angiography with elliptical centric k-space ordering of supra-aortic arteries compared with selective X-ray angiography. *Stroke* 2002;33:1522–1529
- Scarabino T, Carriero A, Giannatempo GM, et al. Contrast-enhanced MR angiography (CE MRA) in the study of carotid stenosis: comparison with digital subtraction angiography (DSA). *J Neuroradiol* 1999;25:87–91
- Modaresi KB, Cox TC, Summers PE, et al. Comparison of intra-arterial digital subtraction angiography, magnetic resonance angiography and duplex ultrasonography for measuring carotid artery stenosis. *Br J Surg* 1999;86:1422–1426
- Carriero A, Scarabino T, Magarelli N, et al. High-resolution magnetic resonance angiography of the internal carotid artery: 2D vs 3D TOF in stenotic disease. *Eur Radiol* 1998;8:1370–1372
- Patel M, Kuntz K, Klufas R, et al. Preoperative assessment of the carotid bifurcation: can magnetic resonance angiography and duplex ultrasonography replace contrast arteriography. *Stroke* 1995;26:1753–1757
- Polak J, Kalina P, Donaldson M, et al. Carotid endarterectomy: preoperative evaluation of candidates with combined doppler sonography and MR angiography. *Radiology* 1993;186:333–338
- Polak J, Bajakian R, O'Leary D, et al. Detection of internal carotid artery stenosis: comparison of MR angiography, color doppler sonography and arteriography. *Radiology* 1992;182:35–40
- Scarabino T, Carriero A, Magarelli N, et al. MR angiography in carotid stenosis: a comparison of three techniques. *Eur J Radiol* 1998;28:117–125
- Leclerc X, Gauvrit J, Nicol L, Pruvo J. Contrast-enhanced MR angiography of the craniocervical vessels: a review. *Neuroradiology* 1999;41:867–874
- Leclerc X, Nicol L, Gauvrit J, et al. Contrast-enhanced MR angiography of supra-aortic vessels: the effect of voxel size on image quality. *AJNR Am J Neuroradiol* 2000;21:1021–1027
- Kollias SS, Blinkert CA, Ruesch S, Valavanis A. Contrast-enhanced MR angiography of the supra-aortic vessels in 24 seconds: a feasibility study. *Neuroradiology* 1999;41:391–400
- Wetzel S, Bongartz G. MR angiography: supra-aortic vessels. *Eur Radiol* 1999;9:1277–1284
- Cosottini M, Pingitore A, Puglioli M, et al. Contrast-enhanced three-dimensional magnetic resonance angiography of atherosclerotic internal carotid stenosis as the noninvasive imaging modality in revascularization decision making. *Stroke* 2003;34:660–664
- Hathout G, Duh M, El-Saden S. Accuracy of contrast-enhanced MR angiography in predicting angiographic stenosis of the inter-

- nal carotid artery: linear regression analysis. *AJNR Am J Neuroradiol* 2003;24:1747-1756
30. Nederkoorn P, Elgersma O, van der Graaf Y, et al. Carotid artery stenosis: accuracy of contrast-enhanced MR angiography for diagnosis. *Radiology* 2003;228:677-682
  31. Lenhart M, Framme N, Volk M, et al. Time-resolved contrast-enhanced magnetic resonance angiography of the carotid arteries: diagnostic accuracy and inter-observer variability compared with selective catheter angiography. *Invest Radiol* 2002;37:535-541
  32. Remonda L, Senn P, Barth A, et al. Contrast-enhanced 3D MR angiography of the carotid artery: comparison with conventional digital subtraction angiography. *AJNR Am J Neuroradiol* 2002;23:213-219
  33. Sundgren P, Sundén P, Lindgren A, et al. Carotid artery stenosis: contrast-enhanced MR angiography with two different scan times compared with digital subtraction angiography. *Neuroradiology* 2002;44:592-599
  34. Aoki S, Nakajima H, Kumagai H, Araki T. Dynamic contrast-enhanced MR angiography and MR imaging of the carotid artery: high-resolution sequences in different acquisition planes. *AJNR Am J Neuroradiol* 2000;21:381-385
  35. Ersoy H, Watts R, Sanelli P, et al. Atherosclerotic disease distribution in carotid and vertebral arteries: clinical experience in 100 patients undergoing fluoro-triggered 3D Gd-MRA. *J Magn Reson Imaging* 2003;17:545-558
  36. Carr J, Ma J, Deshpande V, et al. High-resolution breath-hold contrast-enhanced MR angiography of the entire carotid circulation. *AJR Am J Roentgenol* 2002;178:543-549
  37. Phan T, Huston J 3rd, Bernstein M, et al. Contrast-enhanced magnetic resonance angiography of the cervical vessels: experience with 422 patients. *Stroke* 2001;32:2282-2286
  38. Leclerc X, Lucas C, Godefroy O, et al. Preliminary experience using contrast-enhanced MR angiography to assess vertebral artery structure for the follow-up of suspected dissection. *AJNR Am J Neuroradiol* 1999;20:1482-1490
  39. Hollingworth W, Nathens A, Kanne J, et al. The diagnostic accuracy of computed tomography angiography for traumatic or atherosclerotic lesions of the carotid and vertebral arteries: a systematic review. *Eur J Radiol* 2003;48:88-102
  40. Graf J, Skutta B, Kuhn F, Ferbert A. Computed tomographic angiography findings in 103 patients following vascular events in the posterior circulation: potential and clinical relevance. *J Neurol* 2000;247:760-766
  41. Long A, Lepoutre A, Corbillon E, Branchereau A. Critical review of non- or minimally invasive methods (duplex ultrasonography, MR- and CT-angiography) for evaluating stenosis of the proximal internal carotid artery. *Eur J Vasc Endovasc Surg* 2002;24:43-52
  42. Patel SG, Collie DA, Wardlaw JM, et al. Outcome, observer reliability, and patient preferences if CTA, MRA, or Doppler ultrasound were used, individually or together, instead of digital subtraction angiography before carotid endarterectomy. *J Neurol Neurosurg Psychiatry* 2002;73:21-28
  43. Riles T, Eidelman E, Litt A, et al. Comparison of magnetic resonance angiography, conventional angiography and duplex scanning. *Stroke* 1992;23:341-346
  44. Huston J, Lewis B, Wiebers D, et al. Carotid artery: prospective blinded comparison of two-dimensional time-of-flight MR angiography with conventional angiography and duplex US. *Radiology* 1993;186:339-344
  45. Wentz K, Rother J, Schwartz A, et al. Intracranial vertebrobasilar system: MR angiography. *Radiology* 1994;190:105-110
  46. Furuya Y, Isoda H, Hasegawa S, et al. Magnetic resonance angiography of extracranial carotid and vertebral arteries, including their origins: comparison with digital subtraction angiography. *Neuroradiology* 1992;35:42-45
  47. Bhadelia R, Bengoa F, Gesner L, et al. Efficacy of MR angiography in the detection and characterization of occlusive disease in the vertebrobasilar system. *J Comput Assist Tomogr* 2001;25:458-465
  48. Craig D, Meguro K, Watridge C, et al. Intracranial internal carotid artery stenosis. *Stroke* 1982;13:825-834
  49. Kappelle L, Eliasziw M, Fox A, et al. Importance of intracranial atherosclerotic disease in patients with symptomatic stenosis of the internal carotid artery. *Stroke* 1999;30:282-286
  50. Marzewski D, Furlan A, St Louis P, et al. Intracranial internal carotid artery stenosis long-term prognosis. *Stroke* 1982;13:821-824
  51. Roederer G, Langlois Y, Chan A, et al. Is siphon disease important in predicting outcome of carotid endarterectomy? *Arch Surg* 1983;118:1177-1181
  52. Rouleau P, Huston J 3rd, Gilbertson J, et al. Carotid artery tandem lesions: frequency of angiographic detection and consequences for endarterectomy. *AJNR Am J Neuroradiol* 1999;20:621-625
  53. Keagy B, Poole M, Burnham S, Johnson G Jr. Frequency, severity, and physiologic importance of carotid siphon lesions. *J Vasc Surg* 1986;3:511-515
  54. Weimar C, Kley C, Kraywinkel K, et al. Clinical presentation and prognosis of brain stem infarcts: an evaluation of the Stroke Databank of the German Stroke Foundation. *Nervenarzt* 2002;73:166-173
  55. Berguer R, Morasch M, Kline R. A review of 100 consecutive reconstructions of the distal vertebral artery for embolic and hemodynamic disease. *J Vasc Surg* 1998;27:852-859
  56. Berguer R, Flynn L, Kline R, Caplan L. Surgical reconstruction of the extracranial vertebral artery: management and outcome. *J Vasc Surg* 2000;31:9-18
  57. North American Symptomatic Carotid Endarterectomy Trial Collaborators. Beneficial effect of carotid endarterectomy in symptomatic patients with high-grade carotid stenosis. *N Engl J Med* 1991;325:445-453
  58. The (NASCET) North American Symptomatic Carotid Endarterectomy Trial Steering Committee. North American Symptomatic Carotid Endarterectomy Trial: methods, patient characteristics, and progress. *Stroke* 1991;22:711-720
  59. Snidow J, Johnson M, Harris V, et al. Three-dimensional gadolinium-enhanced MR angiography for aortoiliac inflow assessment plus renal artery screening in a single breath hold. *Radiology* 1996;198:725-732
  60. De Cobelli F, Vanzulli A, Sironi S, et al. Renal artery stenosis: evaluation with breath-hold, three-dimensional, dynamic, gadolinium-enhanced versus three-dimensional, phase-contrast MR angiography. *Radiology* 1997;205:689-695
  61. Hany T, Debatin J, Leung D, Pfammatter T. Evaluation of the aortoiliac and renal arteries: comparison of breath-hold, contrast-enhanced, three-dimensional MR angiography with conventional catheter angiography. *Radiology* 1997;204:357-362
  62. Bakker J, Beek F, Beutler J, et al. Renal artery stenosis and accessory renal arteries: accuracy of detection and visualization with gadolinium-enhanced breath-hold MR angiography. *Radiology* 1998;207:497-504
  63. Carr J, Schirf B, Leloudas N, et al. Temporally-resolved pulmonary MRA with GRAPPA at 3T. *ISMRM* 2004;7